

# Personalization Toolkit: Training Free Personalization of Large Vision Language Models

Soroush Seifi\* Vaggelis Dorovatas Daniel Olmeda Reino Rahaf Aljundi  
Toyota Motor Europe

Hoge Wei 33B, 1930, Zaventem, Belgium

{firstname.lastname}@toyota-europe.com

## Abstract

*Personalization of Large Vision-Language Models (LVLMs) involves customizing models to recognize specific users and object instances, and to generate contextually tailored responses. Existing approaches typically rely on time-consuming test-time training for each user or object, making them impractical for real-world deployment, a limitation reflected in current personalization benchmarks, which are focused on object-centric, single-concept evaluations. In this paper, we present a novel training-free approach to LVLM personalization and introduce a comprehensive real-world benchmark designed to rigorously evaluate various aspects of the personalization task. Our method leverages pre-trained vision foundation models to extract distinctive features, applies retrieval-augmented generation (RAG) techniques to identify instances within visual inputs, and employs visual prompting strategies to guide model outputs. Our model-agnostic vision toolkit enables efficient and flexible multi-concept personalization across both images and videos, without any additional training. We achieve state-of-the-art results, surpassing existing training-based methods.*

## 1. Introduction

Large Vision Language Models (LVLMs) [1, 4, 15–17, 28, 31] have demonstrated impressive capabilities

in reasoning about visual content and answering visual questions across various domains. This suggests a great potential for deployment as visual assistants that can aid users in their daily lives. However, current LVLMs are designed to provide generic, user-independent responses and recognize objects at the category level (Fig. 1, left).

The task of personalizing vision-language models was introduced by [2] to enable LVLMs to recognize specific object instances and answer relevant questions accordingly. Existing approaches [2, 20] rely on training for a specific personalized object, diverting the LVLM from its original capabilities and incurring a large compute cost.

In this work, we introduce a training-free approach that builds upon the strengths of pre-trained vision foundation models, the emerging capabilities of LLMs in in-context learning [7] and retrieval-augmented generation (RAG) [12]. Our method localizes instances using open-world object detectors [11, 18, 21] and stores reference instance-level features in memory banks, alongside their name and context. During inference, our retrieval module queries the memory bank and visual-prompts the LVLM. An overview of our approach is shown in Fig. 1.

Furthermore, existing personalization benchmarks primarily focus on object-centric, single-concept tasks, falling short of capturing the complexity of real-world applications. To address this gap, we introduce a novel and challenging benchmark derived from a video personalization dataset.

\*Providing contracted services for Toyota. E-mail address: soroush.seifi@external.toyota-europe.com

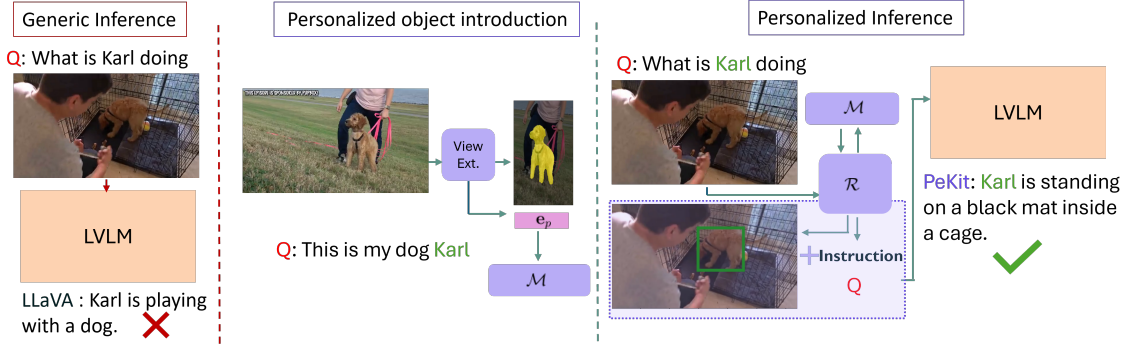


Figure 1. **Illustration of the personalization task and our PeKit.** A reference image is introduced to the LVLM with information and possible context. The LVLM should later be able to answer questions about the introduced object using only the name of the object in the query. Our approach, PeKit, extracts patch-level features from the reference image and stores them in a memory module,  $\mathcal{M}$ . During personalized inference, our retrieval module,  $\mathcal{R}$ , queries  $\mathcal{M}$  to detect the object. PeKit then informs the LVLM via a visual prompt, providing the name and possible context.

It reflects the real-world complexity of the personalization task, with subsets targeting single-concept, multi-concept, image-based, and video-based VQA. We use this benchmark to rigorously evaluate our method across diverse scenarios.

The key contributions of our approach are: 1) We show that LVLM personalization is possible without training, enabling fast deployment. 2) We present a flexible method that supports multi-concept and video personalization across LVLMs using vision foundation models, RAG, and visual prompting. 3) We introduce a challenging benchmark that exposes current limitations and guides future research<sup>1</sup>. 4) We achieve state-of-the-art performance on various tasks using both existing benchmark datasets and our proposed benchmark, consistently surpassing previous methods.

We discuss the related work in Section 2 followed by an introduction to our vision toolkit for LVLMs personalization in Section 3. We then present our real-world benchmark and evaluate our approach in Section 4, and conclude in Section 5.

## 2. Related Work

### Large Vision Language Models Personalization

The task of personalized vision language models was introduced in MyVLM [2] by training a concept head for specific objects on top of the CLIP *cIs* token. In a similar fashion as Dreambooth [25],

MyVLM employs rare tokens to encode personalized concepts. This may have unintended consequences for language assistants, and requires optimizing the LLM caption loss for personalized conversations. Yo’LLaVA [20] adds extra tokens to the LLM head for each personalized object, learning concept tokens to describe them. Although it surpasses MyVLM in performance, the additional tokens create a challenging incremental classification problem [6] when introducing new personalized concepts. Both models need test-time training for each new concept, limiting them to personalizing one concept at a time. Two recent works [9, 22] attempt to eliminate test-time training. While Hao et al. [9] approaches the task by large-scale pretraining on personalized conversations, PLVLM [22] pretrains an alignment module to incorporate the  $\text{CLS}$  token and image embeddings from DINOv2 [21] into the LLM. Hao et al. [9] includes a reference image in the input to the LVLM, which may limit the capability to process multiple images and hinder in-context learning. PLVLM [22] relies on querying for a specific personalized object, limiting its applicability to only VQA. Current approaches are mostly designed for single concept/image personalization and it is unclear how to scale such approaches to more realistic setting. To the contrary, our approach offers a training-free personalization solution, featuring a modular, plug-and-play design that elim-

<sup>1</sup>Our benchmark can be previewed in the supplementary materials and will be made publicly available.



inates the need for retraining or adaptation while naturally and efficiently scaling to multi concept and video personalization.

**Visual Prompting** Visual prompting uses visual cues such as bounding boxes or arrows to guide Vision-Language Models. CLIP [23] interprets these marks to modify its *cls* token embedding accordingly [26]. Set of Mark Prompting [29] integrates GPT-4V with visual prompts using tools like MaskDINO [14], SAM [11], Semantic SAM [13], and SEEM [32]. ViPLLaVA [3] enhances LLaVA [17] to follow visual prompts by tuning on GPT-4V-labeled data. Contrastive Region Grounding (CRG) [27] improves LLaVA’s focus on objects by contrasting token probabilities with and without target object masking. Our experiments show that LLaVA and other LVLMs can describe objects accurately with proper instruction and context. Training-free methods like CRG [27] can further enhance attention if needed.

### 3. Approach

This section outlines our personalization toolkit, coined as *PeKit*, for enabling any LVLM to perform personalized object detection and answer generation. We employ a three-stage pipeline: **View Extraction** to extract robust object-level features from reference images and store them in a memory module, **Personalized Objects Retrieval** to identify objects in the query image, and **Personalized Answer Generation** via visual prompting. We refer to Fig. 1 for an illustration of our approach.

#### 3.1. Preliminary

We consider a set  $P$  of all personalized objects introduced to a given LVLM. Each object  $p \in P$  is associated with a set of reference images  $\{I_p\}$ , a name or identifier  $n_p$  and optionally  $c_p$  a context of the object. Our objective is to generate a personalized response for all images containing  $p$  during inference, while producing a general caption for any other image that does not contain any of the personalized objects. The LVLM, e.g., LLaVA [17] typically takes as input an image  $I_p$ , a text query  $Q$  and additional text as context or instruction.

#### 3.2. Training-free View Extraction

Existing LVLM personalization techniques depend on image-level representations of the objects’ training views [2, 20], which can lead to overfitting to the background of each object in the reference images, particularly for training-based approaches. To avoid such a bias, our method localizes the object in the image and extracts only its corresponding features. We achieve this by utilizing an open-vocabulary segmentation network  $F_{\text{ext}}$  to extract object-level masks  $S_p$  based on each object’s generic category  $k_p$  which can be deduced from the name or the context<sup>2</sup>.

$$S_p = F_{\text{ext}}(I_p, k_p). \quad (1)$$

We construct the average embedding vector  $\mathbf{e}_p$  for object  $p$  by average pooling of the embedding vectors produced by the image encoder  $F_{\text{emb}}$  on the image  $I_p$  over the region defined by the object-level mask  $S_p$ :

$$\mathbf{e}_p = \text{AvgPool}(F_{\text{emb}}(I_p), S_p) \in \mathbb{R}^{D_h}. \quad (2)$$

Considering  $N$  reference images, we concatenate all object embedding vectors  $\mathbf{e}_p^i$  (of the object  $p$  pooled over the  $i$ -th reference image  $I_p^i$ ) into a matrix  $E_p = [\mathbf{e}_p^1, \dots, \mathbf{e}_p^N] \in \mathbb{R}^{D_h \times N}$ .

**Memory module.** After extracting the personalized objects’ embeddings, we store each object’s relevant properties in our memory module. The memory module is represented by a set  $\mathcal{M}$  of object-specific entries:

$$\mathcal{M} = \{(E_p, (n_p, c_p))\}_{p \in P}, \quad (3)$$

where  $n_p$  is the identifier or the name of the personalized object  $p$ , and  $c_p$  is the context of the object, which can contain prior knowledge such as characteristics, background story or even relation to other personalized objects. When the number of personalized objects scales, the memory module  $\mathcal{M}$  is easily converted into a Vector database, where nearest neighbor approximate search is deployed to retrieve instances matching a given query [8] ensuring the efficiency and scalability of our approach.

<sup>2</sup>We refer to Appendix A.5 for further discussion.

### 3.3. Personalized Object Retrieval

During inference, our goal is to determine whether a personalized object is present in the provided image  $I$ . We use any available object proposal technique  $F_{\text{prop}}$  to generate a set of proposals (e.g., bounding boxes)  $O = \{o_i\}_i = F_{\text{prop}}(I)$  for potential object occurrences within the image  $I$ . Then for each proposal  $o_i$ , we calculate its object-level average embedding vector:

$$\mathbf{e}_{o_i} = \text{AvgPool}(F_{\text{emb}}(I), o_i). \quad (4)$$

We define the retrieval module  $\mathcal{R}$  that takes an object embedding vector  $\mathbf{e}_{o_i}$  and retrieves the memory entry  $(E_j, (n_j, c_j))$  for a matching object  $j$  as:

$$\mathcal{R}(\mathbf{e}_{o_i}) = \begin{cases} (E_j, (n_j, c_j)), & \text{if } j = \underset{l}{\text{argmax}} \{ \text{sim}(E_l, \mathbf{e}_{o_i}) \} \\ & \text{and } \text{sim}(E_j, \mathbf{e}_{o_i}) > \tau \\ \phi, & \text{otherwise} \end{cases} \quad (5)$$

where  $\text{sim}(E_l, \mathbf{e}_{o_i}) = \underset{k}{\text{argmax}} \{ \text{sim}(\mathbf{e}_l^k, \mathbf{e}_{o_i}) \}$ . We calculate the proposal’s similarity to the embeddings of the training views for all personalized objects. Any similarity measure (e.g., cosine similarity) can be employed for this purpose. We set a constant threshold  $\tau$  to identify the personalized objects. We discard the object proposals in which no matching object is found by the retrieval module  $\mathcal{R}$ . Our method inherently supports the detection of multiple personalized objects

### 3.4. Personalized Answer Generation

Once a personalized object is identified, our method generates captions specifically about that object, distinct from general captions a standard LVLM would produce. This involves emphasizing the detected object and incorporating prior knowledge about it. We achieve this through visual prompting by overlaying bounding boxes on the image and querying the LVLM to generate captions or answer questions focused on these objects. We use distinctive colors to differentiate recognized objects. We provide the LVLM with the object identifier  $n_j$  (e.g., the instance name) and possibly a context  $c_j$  for each personalized object. The

LVLM incorporates this context and responds to queries using the given name  $n_j$ . For multiple personalized objects, we instruct the LVLM for each bounding box, name, and context. We refer to Appendix C.1 for the exact prompt format.

### 3.5. Video-personalization

To conduct personalized video question answering (VQA), we apply the previously described method to a set of sampled video frames. Each personalized object is consistently highlighted using the same bounding box color across all frames to maintain identity. These sampled frames—including those with visual prompts (bounding boxes) and those without any detected personalized objects—are then fed into a video large language model.

The model is prompted to generate captions or answer questions using each detected object’s identifier  $n_j$ , an optional context  $c_j$ , and the unique bounding box color used for the visual prompting of that object instance (Appendix C.1).

### 3.6. Choice of Vision Tools

We deploy GroundedSAM [24] as the open-vocabulary segmentation network  $F_{\text{ext}}$  and ablate using GroundingDINO [18], where the mask is represented by the object’s bounding box. We use DINOv2 [21] as the image encoder  $F_{\text{emb}}$  to extract patch-level features of the personalized objects. Image encoders trained with a self-supervised objective, such as DINOv2, produce distinctive features that improve the re-identification of personalized objects as we empirically show in Appendix A.1 in a comparison with CLIP [23]. During inference, GroundingDINO [18] is queried with the generic term ‘object’ to generate object proposals.

## 4. Experiments

We present our LVLM personalization validation benchmark and compare our approach with existing personalization methods.

### 4.1. Real-world Personalization Benchmark

Prior personalization datasets such as MyVLM[2] and Yo’LLaVA[20] primarily focus on object-centric scenarios in controlled settings.

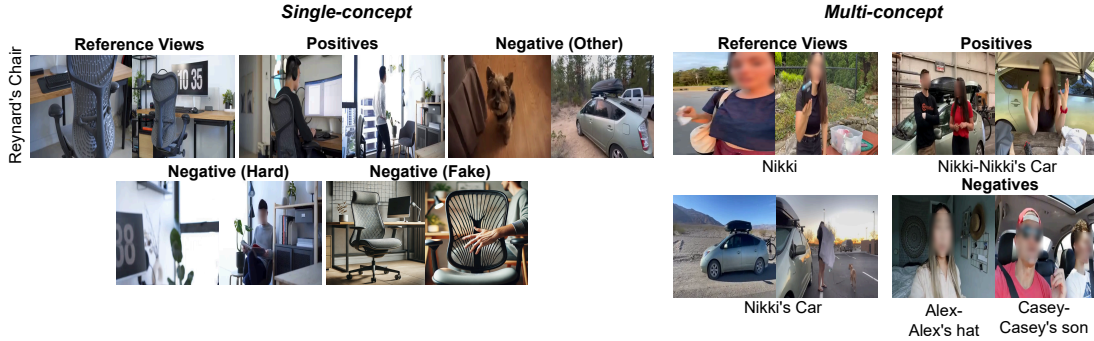


Figure 2. **Our proposed evaluation set This-Is-My-Img, built on the This-Is-My dataset [30]:** Example reference views and validation samples from the single-concept category *Reynard's Work Chair* and the multi-concept category *Nikki-Nikki's Car*. Faces are blurred to ensure compliance with GDPR.

**MyVLM** [2] dataset consists of 29 object categories and **Yo'LLaVA** [20] dataset includes 40 categories of objects, buildings, and people. It also features a VQA benchmark with multiple-choice questions (A/B). Despite their utility, these datasets lack real-world complexity—such as background clutter, partial occlusions, and diverse contexts—limiting their effectiveness for evaluating robust LVLm personalization.

To address this gap, we introduce a more realistic evaluation set called **This-Is-My-Img** benchmark, based on the *This-Is-My* dataset [30], originally developed for video-level detection of personalized instances in realistic settings where objects may be partially occluded, in the background, or poorly lit. We design several splits to evaluate specific capabilities of personalization methods.

**Reference Views:** As in prior work, we extract five reference images per object from training segments. Unlike earlier datasets, objects in these frames may appear under suboptimal conditions—e.g., partially visible, in the background, or poorly lit (Fig. 3 Appendix).

**Single-Concept Eval Set:** Set of images with a single personalized object. Fig. 2 shows examples. For each personalized object, images are labeled as:

- *Positive:* Contain the personalized object and are used to evaluate the method's recall performance.
- *Negative-Hard:* Taken from validation segments of the same object where the object is not visible. This tests methods's overfitting to the background associated with the personalized object.

- *Negative-Other:* Sourced from validation segments of other personalized objects. Measures method's robustness to intra-instance and the general dataset bias.
- *Negative-Fake:* AI-generated images (via GPT) that mimic the personalized object under varied perspectives and environments. These samples are used to assess the method's robustness against high visual similarity combined with a distribution shift.
- *Single-Concept VQA:* A set of A/B multiple-choice questions based on positive images, in Yo'LLaVA-style format.

**Multi-Concept Set:** Images including a pair of personalized concepts. For example a person-object pair (Nikki & Nikki's car) or a person-person pair (Casey & Casey's son). To achieve this, we extend the personalized instances of the original dataset. Positives of a pair of personalized objects are images with both instances of the pair appearing together while negatives include all images from other pairs in the dataset. See Fig. 2 for examples.

- *Multi-Concept VQA:* Provides open-ended questions for each image in the multi-concept set that address both objects depicted.

**Video-QA Set:** Original video clips from the *This-Is-My* dataset are paired with open-ended questions about the personalized object in the video, testing both temporal reasoning and the method's adaptability to video inputs.

Our evaluation benchmark presents a comprehensive challenge for LVLm personalization, requiring

recognition and reasoning over personalized objects in realistic, cluttered, and dynamic conditions. Appendix.B presents more details on each set.

## 4.2. Metrics and Evaluation Setting

**Single-Concept Metrics.** We follow the metrics and notation of Yo’LLaVA [20] and MyVLM [2], reporting *Positive Accuracy* (Recall), *Negative Accuracy* (Specificity) and *Weighted Accuracy* for  $n$  personalized objects. We further report *Precision*, defined as the ratio of true positive predictions to the total number of instances predicted as positive, averaged over  $n$  personalized objects. We believe this is a more comprehensive evaluation recognizing the trade-off between the aforementioned metrics and precision. VQA accuracy on single-concept datasets is measured as the percentage of correctly selected multiple-choice questions. In line with MyVLM, we also report *CLIPScore*, which evaluates the similarity between the generated caption and the image, and *Personalization Recall*, which measures how effectively the model incorporates the personalized object’s name into the caption on the MyVLM dataset.

**Multi-Concept Metrics.** Positive accuracy is measured as to number of times when both personalized objects in the image are correctly detected. Negative accuracy is measured as the number of times at least one of the two objects are correctly **not** detected in an image.

**Video and Multi-concept VQA Metric.** For open-ended VQA validation, we follow a protocol similar to that of [19], utilizing ChatGPT-3.5 to evaluate the accuracy of the model’s responses (see Appendix C.2 for more details).

**Implementation Details.** The modularity of our method makes it generic regarding the choice of the LVLM model. We use LLaVA1.5-13B [16] as our primary LVLM model for consistency with previous works. We pair PeKit with InternVL2-26B [4], a state-of-the-art LVLM to ablate. We use LLaVA-OneVision-Qwen2-7B as our default video model and ablate with InternVideoChat2.5 as a superior video model. We utilize Cosine Similarity with a constant threshold of  $\tau=0.75$  for detecting personalized objects across all datasets (3.3). Refer to

MyVLM Dataset				
Method/Metric	Precision	Accuracy		
		Positive	Negative	Weighted
MyVLM [2]	-	96.6	90.9	93.8
Yo’ LLaVA [20]	-	97.0	95.7	96.4
PeKit (G-DINO)	79.1	94.3	98.8	96.55
PeKit (G-SAM)	82.3	97.6	99	98.3
Yo’ LLaVA Dataset				
Yo’ LLaVA [20]	-	94.9	89.8	92.4
PeKit (G-DINO)	77	89.9	98.9	94.4
PeKit (G-SAM)	74.8	91	98.7	94.9

Table 1. Visual Recognition performance on MyVLM and YoLLaVA datasets. Our approach PeKit achieves state of the art performance and improves significantly over existing methods.

This-Is-My-Img Single-Concept Dataset						
Method/Metric	Precision	Positive	Accuracy			Avg.
			Other	Hard	Fake	
MyVLM	8.0	<b>88.1</b>	14.6	4.7	54.2	33.9
Yo’LLaVA	42.1	87.1	84.4	61.9	<b>61.4</b>	67.3
PeKit	<b>90.1</b>	69.0	<b>99.9</b>	<b>96.0</b>	59.3	<b>82.8</b>

This-Is-My-Img Multi-Concept Dataset				
Method/Metric	Precision	Accuracy		Avg.
		Positive	Negative	
Yo’LLaVA	10.0	<b>83.6</b>	25.0	54.3
PeKit	<b>96.1</b>	45.4	<b>99.8</b>	<b>72.6</b>

Table 2. Visual Recognition Performance (%) on This-Is-My-Img dataset. MyVLM and Yo’LLaVA tend to capture the dataset’s bias and produces many false positives when the images are taken from similar scenes regardless of the object’s presence.

Appendix A.7 for further details on compute and memory overhead of our personalization toolkit.

## 4.3. Visual-Recognition

**Previous Datasets** Tab. 1 compares our method to MyVLM [2] and Yo’LLaVA [20] on their respective benchmarks. On MyVLM, PeKit achieves a new SOTA, improving both positive and negative accuracy with an average gain of 1.9%. On Yo’LLaVA, it increases negative accuracy by 8.9%, with slightly lower positive accuracy, resulting in a SOTA 2.5% improvement in weighted accuracy. While PeKit may miss some difficult instances, its low false positive rate helps avoid incorrect personalized outputs, favoring generic captions when uncertain. We ablate the choice of an open-world object detector, G-DINO [18], compared to the open-world semantic segmentation model, G-SAM [24],

Method	Metric	
	CLIPScore	Personal. Recall
MyVLM Dataset		
MyVLM [2]	<u>27.6</u>	<u>94.76</u>
PeKit (LLaVA)	<b>30.2</b>	<b>97.1</b>
Method	Metric	
	VQA Accuracy	
Yo'LLaVA Dataset		
LLaVA [20]	89.9	
Yo'LLaVA [20]	92.9	
PeKit (LLaVA)	<u>93.4</u>	
PeKit (InternVL)	<b>95.9</b>	
This-Is-My-Img Single-Concept Dataset		
LLaVA	72.8	
Yo'LLaVA	67.1	
PeKit (LLaVA)	<u>77.1</u>	
PeKit (InternVL)	<b>84.2</b>	
This-Is-My-Img Multi-Concept Dataset		
LLaVA	49.0	
Yo'LLaVA	12.7	
PeKit (LLaVA)	<u>56.3</u>	
PeKit (InternVL)	<b>63.6</b>	
This-Is-My-Video Dataset		
LLaVA-OneVision-Qwen2	23.0	
InternVideoChat2.5	<u>56.6</u>	
PeKit (LLaVA-OneVision-Qwen2)	35.0	
PeKit (InternVideoChat2.5)	<b>61.3</b>	

Table 3. Visual Question Answering Performance. PeKit achieves SOTA performance on all benchmarks.

for  $F_{\text{ext}}$  in Eq. 1. The results show that our method outperforms previous methods in both cases. However, the more precise segmentation model, which extracts only patches of the object of interest, achieves the best accuracy on average.

**This-Is-My-Img Benchmark.** Tab. 2 reports the performance on our benchmark. For single-concept images, **MyVLM** shows high positive accuracy but poor negative accuracy (14.6% on *other* and 4.7% on *hard* negatives), suggesting it focuses on scene context over specific objects and tends to provide mostly positive responses to test images. **Yo'LLaVA** performs similarly but better, with 87.1% positive accuracy and 84.8% on *other* and 61.9% on *hard* negative samples. In contrast, **PeKit** offers stronger negative accuracy (99.9% and 96.0%) with a precision of 90.1%—48% higher than Yo'LLaVA—indicating fewer false positives.

On fake images, differences narrow. All models struggle with objects stylistically close to the personalized one with image-level methods like MyVLM and Yo'LLaVA potentially having a

higher chance to detect the domain shift. However, PeKit also demonstrates robustness to domain variations, despite some difficulty with highly similar objects. Overall, PeKit achieves the best balance, with an average accuracy of 82.86%, outperforming Yo'LLaVA (67.38) and MyVLM (33.92).

In multi-concept settings, PeKit shows slightly lower accuracy in dual-object detection but achieves much higher precision and negative accuracy, leading to an 18.3% overall accuracy gain over Yo'LLaVA. These results highlight our training-free method's superior robustness and lower false positive rate, especially in complex real-world scenarios.

Overall, this evaluation set illustrates the difficulty of the personalization task beyond object-centric images, moving closer to realistic scenarios for intelligent visual assistants. This opens the door for future research on this challenging benchmark.

#### 4.4. Visual-Question Answering

In Tab. 3, we assess PeKit performance in answering questions about personalized objects across various scenarios. We evaluate our approach using the Yo'LLaVA [20] and This-Is-My-Img benchmarks. For a comprehensive comparison, we also evaluate PeKit against MyVLM on the MyVLM dataset using CLIPScore [10] and Personalization Recall.

Our method consistently outperforms baseline models on both single- and multi-concept VQA tasks. On the MyVLM dataset, PeKit surpasses the MyVLM method in generating image-aligned captions (as measured by CLIPScore) and in correctly incorporating personalized concept names (as measured by Personalization Recall). On the Yo'LLaVA dataset, PeKit outperforms Yo'LLaVA despite requiring no additional training, special tokens, or modifications to the original LVLM.

On the This-Is-My-Img benchmark, Yo'LLaVA fails to improve over the base LLaVA model, whereas PeKit achieves a notable performance gain of approximately 5%, demonstrating strong capabilities in both visual recognition and question answering. Additionally, PeKit generalizes well to the video domain (3.5), unlike prior approaches, which are not readily extendable to video. In this setting, our method improves the original



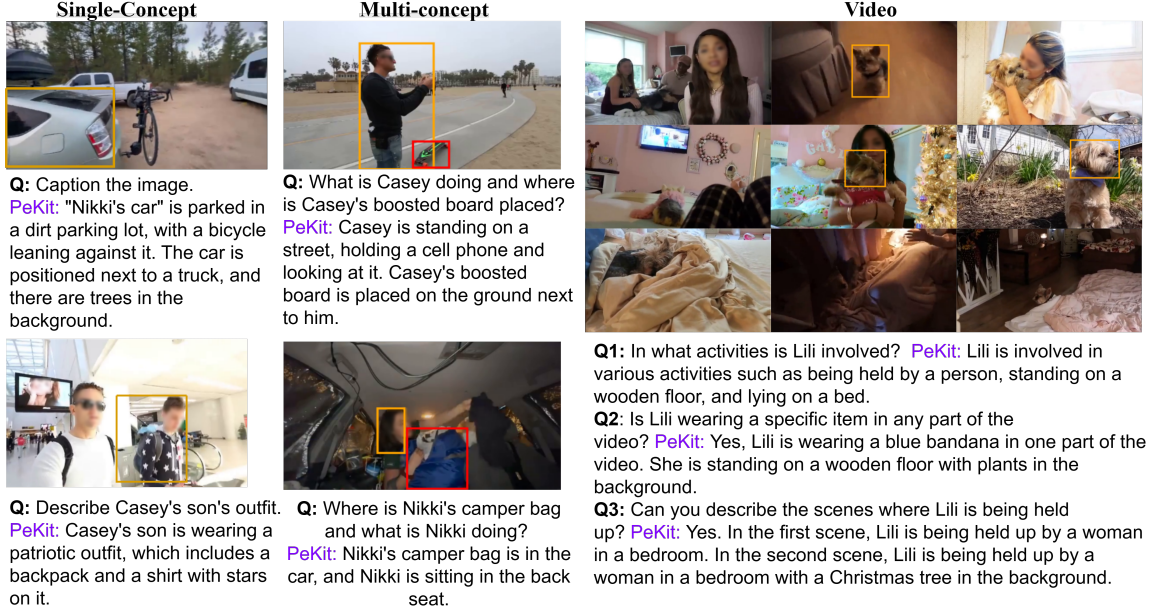


Figure 3. **Qualitative Results:** PeKit handles a range of personalization tasks, encompassing both single- and multi-concept personalization in images and videos. For video personalization, the VLM model can reliably track the target object across frames using only a few confidently annotated instances. One representative frame is shown per scene. Faces are blurred to ensure compliance with GDPR.

model’s performance by 12% and continue to show gains when paired with a more capable instruction-following backbone.

#### 4.5. Qualitative Results

Fig. 3 presents examples of our PeKit model performing various tasks on the proposed benchmark, This-Is-My-Img. In the left column, PeKit successfully identifies personalized single-concept objects, even in ambiguous scenarios involving multiple instances from the same object category. In the middle column, it demonstrates the ability to answer questions involving multi-concept pairs. Lastly, without any modifications, the model can be applied to video inputs by visually prompting the model with detected personalized objects in the video. Additional qualitative comparisons with the base LLaVA model, MyVLM, and Yo’LLaVA are provided in Appendices E, F, and G.

#### 4.6. Ablation and Analysis

A comprehensive evaluation of our method is provided in Appendix.A, where we analyze robustness under various settings. Specifically, we examine the effects of altering the backbone encoder  $F_{emb}$ , the number of reference images per object ( $N$ ), the

number of personalized objects ( $P$ ) in the dataset, the detection threshold ( $\tau$ ), semantic category ( $k_p$ ) and the name ( $n_p$ ) of the personalized objects.

#### 5. Discussion and Conclusion

In this work, we introduced PeKit, a training-free, plug-and-play toolkit for LVLM personalization that combines vision foundation models with retrieval-augmented generation and visual prompting. Our approach outperforms existing training-based methods without requiring any fine-tuning or additional data beyond the personalized concept inputs. To evaluate our method, we proposed a challenging new benchmark that reflects more realistic scenarios involving multi-concept and video personalization, significantly increasing the complexity of the visual recognition task. PeKit demonstrates strong robustness and scalability across both multi-concept and video settings. Despite its strengths, our benchmark reveals that there is still room for improvement, particularly in handling complex temporal and multi-concept reasoning. We believe that PeKit establishes a strong training-free baseline for future research in LVLM personalization.

## References

- [1] Pravesh Agrawal, Szymon Antoniak, Emma Bou Hanna, Baptiste Bout, Devendra Chaplot, Jessica Chudnovsky, Diogo Costa, Baudouin De Monicault, Saurabh Garg, Theophile Gervet, Soham Ghosh, Amélie Héliou, Paul Jacob, Albert Q. Jiang, Kartik Khandelwal, Timothée Lacroix, Guillaume Lample, Diego Las Casas, Thibaut Lavril, Teven Le Scao, Andy Lo, William Marshall, Louis Martin, Arthur Mensch, Pavankumar Muddireddy, Valera Nemychnikova, Marie Pellat, Patrick Von Platen, Nikhil Raghuraman, Baptiste Rozière, Alexandre Sablayrolles, Lucile Saulnier, Romain Sauvestre, Wendy Shang, Roman Soletskyi, Lawrence Stewart, Pierre Stock, Joachim Studnia, Sandeep Subramanian, Sagar Vaze, Thomas Wang, and Sophia Yang. Pixtral 12b, 2024. [1](#)
- [2] Yuval Alaluf, Elad Richardson, Sergey Tulyakov, Kfir Aberman, and Daniel Cohen-Or. Myvlm: Personalizing vlms for user-specific queries. *arXiv preprint arXiv:2403.14599*, 2024. [1](#), [2](#), [3](#), [4](#), [5](#), [6](#), [7](#), [18](#)
- [3] Mu Cai, Haotian Liu, Siva Karthik Mustikovela, Gregory P Meyer, Yuning Chai, Dennis Park, and Yong Jae Lee. Vip-llava: Making large multi-modal models understand arbitrary visual prompts. In *Proceedings of the IEEE/CVF Conference on Computer Vision and Pattern Recognition*, pages 12914–12923, 2024. [3](#)
- [4] Zhe Chen, Jiannan Wu, Wenhai Wang, Weijie Su, Guo Chen, Sen Xing, Muyan Zhong, Qinglong Zhang, Xizhou Zhu, Lewei Lu, et al. Internvl: Scaling up vision foundation models and aligning for generic visual-linguistic tasks. In *Proceedings of the IEEE/CVF Conference on Computer Vision and Pattern Recognition*, pages 24185–24198, 2024. [1](#), [6](#)
- [5] Tianheng Cheng, Lin Song, Yixiao Ge, Wenyu Liu, Xinggang Wang, and Ying Shan. Yolo-world: Real-time open-vocabulary object detection. In *Proc. IEEE Conf. Computer Vision and Pattern Recognition (CVPR)*, 2024. [12](#)
- [6] Matthias De Lange, Rahaf Aljundi, Marc Masana, Sarah Parisot, Xu Jia, Aleš Leonardis, Gregory Slabaugh, and Tinne Tuytelaars. A continual learning survey: Defying forgetting in classification tasks. *IEEE transactions on pattern analysis and machine intelligence*, 44(7):3366–3385, 2021. [2](#)
- [7] Qingxiu Dong, Lei Li, Damai Dai, Ce Zheng, Jingyuan Ma, Rui Li, Heming Xia, Jingjing Xu, Zhiyong Wu, Baobao Chang, et al. A survey on in-context learning. In *Proceedings of the 2024 Conference on Empirical Methods in Natural Language Processing*, pages 1107–1128, 2024. [1](#)
- [8] Yikun Han, Chunjiang Liu, and Pengfei Wang. A comprehensive survey on vector database: Storage and retrieval technique, challenge. *arXiv preprint arXiv:2310.11703*, 2023. [3](#)
- [9] Haoran Hao, Jiaming Han, Changsheng Li, Yufeng Li, and Xiangyu Yue. Remember, retrieve and generate: Understanding infinite visual concepts as your personalized assistant, 2024. [2](#)
- [10] Jack Hessel, Ari Holtzman, Maxwell Forbes, Roman Le Bras, and Yejin Choi. Clipscore: A reference-free evaluation metric for image captioning. *arXiv preprint arXiv:2104.08718*, 2021. [7](#)
- [11] Alexander Kirillov, Eric Mintun, Nikhila Ravi, Hanzi Mao, Chloe Rolland, Laura Gustafson, Tete Xiao, Spencer Whitehead, Alexander C Berg, Wan-Yen Lo, et al. Segment anything. In *Proceedings of the IEEE/CVF International Conference on Computer Vision*, pages 4015–4026, 2023. [1](#), [3](#), [12](#)
- [12] Patrick Lewis, Ethan Perez, Aleksandra Piktus, Fabio Petroni, Vladimir Karpukhin, Naman Goyal, Heinrich Küttler, Mike Lewis, Wen-tau Yih, Tim Rocktäschel, et al. Retrieval-augmented generation for knowledge-intensive nlp tasks. *Advances in Neural Information Processing Systems*, 33:9459–9474, 2020. [1](#)
- [13] Feng Li, Hao Zhang, Peize Sun, Xueyan Zou, Shilong Liu, Jianwei Yang, Chunyuan Li, Lei Zhang, and Jianfeng Gao. Semantic-sam: Segment and recognize anything at any granularity. *arXiv preprint arXiv:2307.04767*, 2023. [3](#)
- [14] Feng Li, Hao Zhang, Huaizhe Xu, Shilong Liu, Lei Zhang, Lionel M Ni, and Heung-Yeung Shum. Mask dino: Towards a unified transformer-based framework for object detection and segmentation. In *Proceedings of the IEEE/CVF Conference on Computer Vision and Pattern Recognition*, pages 3041–3050, 2023. [3](#)
- [15] Junnan Li, Dongxu Li, Silvio Savarese, and Steven Hoi. Blip-2: Bootstrapping language-image pre-training with frozen image encoders and large language models. In *International conference on machine learning*, pages 19730–19742. PMLR, 2023. [1](#)
- [16] Haotian Liu, Chunyuan Li, Yuheng Li, and Yong Jae Lee. Improved baselines with visual instruction tuning. In *Proceedings of the*

- IEEE/CVF Conference on Computer Vision and Pattern Recognition*, pages 26296–26306, 2023. 6
- [17] Haotian Liu, Chunyuan Li, Qingyang Wu, and Yong Jae Lee. Visual instruction tuning. *Advances in neural information processing systems*, 36, 2023. 1, 3, 16
- [18] Shilong Liu, Zhaoyang Zeng, Tianhe Ren, Feng Li, Hao Zhang, Jie Yang, Qing Jiang, Chunyuan Li, Jianwei Yang, Hang Su, et al. Grounding dino: Marrying dino with grounded pre-training for open-set object detection. *arXiv preprint arXiv:2303.05499*, 2023. 1, 4, 6, 12
- [19] Muhammad Maaz, Hanoona Rasheed, Salman Khan, and Fahad Shahbaz Khan. Video-chatgpt: Towards detailed video understanding via large vision and language models. *arXiv preprint arXiv:2306.05424*, 2023. 6, 15
- [20] Thao Nguyen, Haotian Liu, Yuheng Li, Mu Cai, Utkarsh Ojha, and Yong Jae Lee. Yo’llava: Your personalized language and vision assistant. *arXiv preprint arXiv:2406.09400*, 2024. 1, 2, 3, 4, 5, 6, 7, 11, 18
- [21] Maxime Oquab, Timothée Darcet, Théo Moutakanni, Huy Vo, Marc Szafraniec, Vasil Khalidov, Pierre Fernandez, Daniel Haziza, Francisco Massa, Alaaeldin El-Nouby, et al. Dinov2: Learning robust visual features without supervision. *arXiv preprint arXiv:2304.07193*, 2023. 1, 2, 4
- [22] Chau Pham, Hoang Phan, David Doermann, and Yunjie Tian. Personalized large vision-language models, 2024. 2
- [23] Alec Radford, Jong Wook Kim, Chris Hallacy, Aditya Ramesh, Gabriel Goh, Sandhini Agarwal, Girish Sastry, Amanda Askell, Pamela Mishkin, Jack Clark, et al. Learning transferable visual models from natural language supervision. In *International conference on machine learning*, pages 8748–8763. PMLR, 2021. 3, 4
- [24] Tianhe Ren, Shilong Liu, Ailing Zeng, Jing Lin, Kunchang Li, He Cao, Jiayu Chen, Xinyu Huang, Yukang Chen, Feng Yan, et al. Grounded sam: Assembling open-world models for diverse visual tasks. *arXiv preprint arXiv:2401.14159*, 2024. 4, 6
- [25] Nataniel Ruiz, Yuanzhen Li, Varun Jampani, Yael Pritch, Michael Rubinstein, and Kfir Aberman. Dreambooth: Fine tuning text-to-image diffusion models for subject-driven generation. In *Proceedings of the IEEE/CVF conference on computer vision and pattern recognition*, pages 22500–22510, 2023. 2
- [26] Aleksandar Shtedritski, Christian Rupprecht, and Andrea Vedaldi. What does clip know about a red circle? visual prompt engineering for vlms. In *Proceedings of the IEEE/CVF International Conference on Computer Vision*, pages 11987–11997, 2023. 3
- [27] David Wan, Jaemin Cho, Elias Stengel-Eskin, and Mohit Bansal. Contrastive region guidance: Improving grounding in vision-language models without training. In *ECCV*, 2024. 3
- [28] Peng Wang, Shuai Bai, Sinan Tan, Shijie Wang, Zhihao Fan, Jinze Bai, Keqin Chen, Xuejing Liu, Jialin Wang, Wenbin Ge, et al. Qwen2-vl: Enhancing vision-language model’s perception of the world at any resolution. *arXiv preprint arXiv:2409.12191*, 2024. 1
- [29] Jianwei Yang, Hao Zhang, Feng Li, Xueyan Zou, Chunyuan Li, and Jianfeng Gao. Set-of-mark prompting unleashes extraordinary visual grounding in gpt-4v. *arXiv preprint arXiv:2310.11441*, 2023. 3
- [30] Chun-Hsiao Yeh, Bryan Russell, Josef Sivic, Fabian Caba Heilbron, and Simon Jenni. Meta-personalizing vision-language models to find named instances in video. In *Proceedings of the IEEE/CVF Conference on Computer Vision and Pattern Recognition*, pages 19123–19132, 2023. 5, 13
- [31] Deyao Zhu, Jun Chen, Xiaoqian Shen, Xiang Li, and Mohamed Elhoseiny. Minigpt-4: Enhancing vision-language understanding with advanced large language models. *arXiv preprint arXiv:2304.10592*, 2023. 1
- [32] Xueyan Zou, Jianwei Yang, Hao Zhang, Feng Li, Linjie Li, Jianfeng Wang, Lijuan Wang, Jianfeng Gao, and Yong Jae Lee. Segment everything everywhere all at once. *Advances in Neural Information Processing Systems*, 36, 2024. 3

## A. Ablation

In this section we ablate various aspects of our personalization method primarily using the Yo’LLaVA dataset as it serves as a well-established benchmark.

### A.1. Retrieval Module Backbone

We present an ablation study of the image encoder  $F_{emb}$ , which serves as the backbone of the Retrieval Module and is responsible for extracting object features and performing matching. We observe a noticeable gap between CLIP and DINO, indicating that DINO’s visual features are more discriminative and better suited for retrieval tasks. Between the two DINO variants (base and large), the larger version delivers slightly better performance, the difference is marginal indicating that any DINOv2 backbone can be deployed.

Yo’ LLaVA Dataset				
Method/Metric	Precision	Recall		
		Positive	Negative	Weighted
DINOv2 (Large)	74.8	<b>91</b>	<b>98.7</b>	<b>94.9</b>
DINOv2 (Base)	<b>75.5</b>	90.8	<b>98.7</b>	<b>94.7</b>
CLIP (Large)	69	78.3	98.2	88.3

Table 4. **Feature Extractor Ablation.** We observe that DINO features significantly outperform CLIP features.

### A.2. Number of Reference Images ( $N$ )

Since our approach does not require a training phase, a key question is how many reference images are needed for robust visual recognition of personalized objects. Figure 4 shows that our method performs well with just one reference image and matches state-of-the-art performance with two images on MyVLM dataset. On Yo’LLaVA dataset, we achieve comparable performance to Yo’LLaVa [20] with only three images, even though the full set includes up to 10 images for some objects.

### A.3. Number of Personalized Objects ( $P$ )

Another key consideration for any personalization method is its robustness to increasing number of personalized objects, particularly as more intra-category instances are introduced into the dataset. Figure 5 illustrates the performance of PeKit on

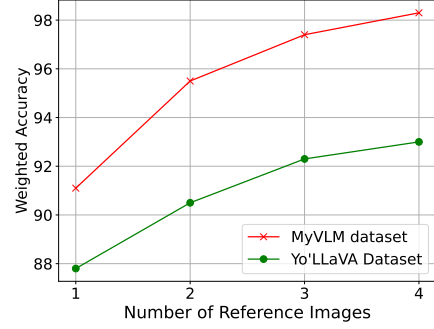


Figure 4. **Ablation on  $N$ :** Average weighted visual recognition accuracy as a function of number of reference images. Increasing the number of reference images improves performance, but PeKit is robust with just one reference image.

the first 10 objects from the Yo’LLaVA dataset as the number of personalized objects increases incrementally from 10 to all 40 categories. While there is a slight performance drop at higher values of  $P$ , PeKit demonstrates overall stability and robustness.

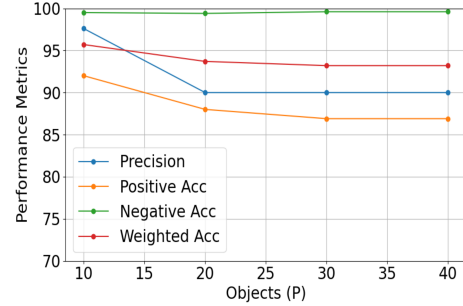


Figure 5. **Ablation on  $P$ :** PeKit’s performance when evaluated on a subset of 10 categories from Yo’LLaVA dataset while progressively increasing number of objects.

### A.4. Threshold Selection

In the main paper, we used a fixed threshold of 0.75 for all settings in order to decide whether a personalized object is present in an image or not. For completeness and flexibility, here we offer a straightforward method for tuning the thresholds on a per-object basis. To adjust the threshold for a given personalized object  $i$ , we first compute the distribution of distances for the reference images of the object, and then calculate the mean  $\mu_i$  and standard devi-

ation  $\sigma_i$  of the distribution. The threshold is then set as  $\tau_i = \mu_i - \sigma_i/2$ . (We note that by using this method, one can easily adjust the thresholds to be stricter or more loose by adding a scalar multiplier, as  $\tau_i = \mu_i - \alpha(\sigma_i/2)$ .)

Yo' LLaVA Dataset				
Method/Metric	Precision	Recall		
		Positive	Negative	Weighted
Fixed $\tau = 0.75$	<b>74.8</b>	91	<b>98.7</b>	94.9
Tuned $\tau = \mu - \sigma/2$	66	<b>92.5</b>	98.1	<b>95.3</b>

Table 5. Automatic object threshold selection.

### A.5. Semantic Category

As mentioned in Section 3.2 of the main paper, we employ each object’s semantic category  $k_p$  on the reference image  $I_p$  to extract its object-level mask  $S_p$ . For the MyVLM dataset, where the object names are generic, we directly input them into our open-vocabulary detector. Similarly, on This-Is-My-Img dataset, aside from the people in the dataset (queried with the category ‘Man/Woman’), all other object names in this dataset include their semantic category (e.g., Alex’s hat, See Appendix.B).

For the Yo’LLaVA dataset, some concept names such as Vietnamese individual names do not directly indicate the semantic categories. We compare our method’s performance on the Yo’LLaVA dataset by providing the open-vocabulary segmentation model with semantic categories, dataset-provided names, or the generic term ‘main’ during reference view extraction. As shown in Table 6, PeKit achieves state-of-the-art performance even without relying on semantic categories of personalized objects. Note that during inference we consistently use the term ‘object’ to extract object proposals using G-Dino.

Method/Metric	Precision	Positive Acc	Negative Acc	Weighted Acc
Yo’ LLaVA	-	<b>94.9</b>	89.8	92.4
PeKit (categories)	<b>74.8</b>	91	98.7	<b>94.9</b>
PeKit (‘main’)	72.9	86.9	<b>98.9</b>	92.9
PeKit (Vietnamese names)	73.8	88	<b>98.9</b>	93.45

Table 6. Reference View Vocabulary Ablation on Yo’LLaVA Dataset. Our method achieves SOTA results even using the category ‘main’ to extract the personalized objects from the reference views.

Model/Variation	Base	PeKit	Base+ENTITY	PeKit +ENTITY
LLaVA-OneVision	23.0	<b>35.0</b>	14.0	19.9
InternVideoChat	56.6	<b>61.3</b>	45.8	56.2

Table 7. Example table showing values for different VLM model variations

### A.6. Video-QA Object Naming

Object names often offer important contextual clues about the subject in a query to the base LVLM. For example, when asked “What is Jack doing?”, the model may infer that “Jack” refers to a male individual in the image. In such cases, the LVLM can often respond accurately without the need for personalization. To isolate the effect of personalization, we perform an ablation study on an open-ended video QA task, where all identified personalized objects are visually prompted using the generic label ENTITY (see Appendix C and Fig.7). Table 7 compares our method’s performance when using object names or the term ENTITY to the base LVLM models.

### A.7. Time and Memory Requirements

Table 8 details the memory usage and runtime of the various modules in our method for the LVLM personalization task. By default, we employ GroundingDINO (Base) [18] and SAM (Base) [11] for extracting views from reference images and proposing objects during inference, DINOv2 (Large) features for retrieving personalized instances, and LLaVA 1.5 13B as our LVLM for generating answers. All experiments were conducted using an A5000 RTX GPU. As shown in the table, our plug-and-play modules are efficient, adding minimal overhead to the original LLaVA model.

Specifically, our approach introduces an overhead of 0.35 seconds per image (0.31 seconds from G-DINO) relative to LVLM’s inference time. This overhead can be substantially reduced by employing a lightweight object proposal network such as YOLO-World [5], which runs at 55 FPS compared to G-DINO’s 3 FPS. However, as reducing computational time is not the primary focus of this work, we leave further optimization in this direction for



future research.

Module	Backbone	Time/Image (S)	Memory (GB)
View Extraction	G-DINO + SAM	0.48	1.2
Object Proposal	G-DINO	0.31	0.87
Retrieval	DINOv2	0.04	1.8
Reasoning	LLaVA 1.5 13B	0.87	16.8

Table 8. **Time and Memory Requirement.** View extraction is conducted only on the reference views corresponding to each personalized object category, whereas the remaining modules are executed for every image during inference.

## B. This-Is-My-Img Benchmark Details

The original This-Is-My dataset [30], designed for video-level detection of personalized objects, comprises 104 training and 582 validation short video segments spanning 15 categories. However, some of the segments are no longer available for download. Consequently, one personalized object category, ‘Alex’s Piano’ has been removed from our proposed benchmark due to the unavailability of its training segments.

### B.1. Single-concept Set

Table 9 presents further details about the personalized objects and the number of frames included in the single-concept validation splits of our benchmark. We sampled every 10th frame of each validation video segment and manually assigned frames to the respective splits. Note that three categories lack a **Negative (Hard)** set because the corresponding objects are present in every frame of their validation segments. The number of **Positive**, **Negative (Hard)**, and **Negative (Other)** frames varies between categories due to differences in segment length and the number of segments per object. In contrast, the **Fake** set was standardized, with 10 validation frames generated for each class. Figure 6 offers additional visual examples from our benchmark.

The single-concept validation also includes an open-ended VQA set comprising 70 images (5 per category). Challenging frames were manually selected, and initial question-answer pairs were generated using the GPT-4O model. These pairs were then manually refined to create a high-quality evaluation set. In line with the Yo’LLaVA frame-

work, answers for this set are presented in an A/B multiple-choice format.

Category	Positive	Negative (Hard)	Negative (Other)
Alex’s Bag	161	43	2096
Alex’s Hat	120	0	2137
Blippi’s Shoes	339	79	1918
Casey’s Boosted Board	35	118	2222
Casey’s Friend Marlan	24	4	2233
Casey’s Son	46	15	2211
Gab’s Puppy Lili	56	12	2201
Nikki’s Camper Bag	229	76	2028
Nikki’s Car	651	184	1606
Reynard’s Keyboard	162	29	2095
Reynard’s Work Chair	188	59	2069
Sherry’s Road Bike	95	12	2162
Zak’s Dog Coffee	26	0	2231
Zak’s Dog Kona	125	0	2132
Sum	2257	631	29341

Table 9. **Single-concept Categories and Number of Frames of This-Is-My-Img Benchmark.** The validation frames in the dataset are divided into two sets for each category: one with the object visible (*Hard*) in the image and one without (*Other*). The benchmark also includes a GPT-generated set of 10 images per category (*Fake*).

### B.2. Multi-concept Set

Table 10 outlines the category pairs used in our multi-concept validation benchmark. This benchmark comprises 55 images, with each category pair represented by 5 manually selected positive examples sourced from the validation frames. We extended the original This-Is-My-Img dataset categories (Table 9) by incorporating new personalized categories: Alex, Blippi, Casey, Gab, Nikki, Sherry, and Zak. For each of these added categories, we selected 5 reference views from the training segments. Each image in the benchmark is accompanied by an open-ended question-answer pair, collaboratively crafted with GPT-4O. This open-ended visual question answering (VQA) format raises the task’s difficulty and reduces the likelihood that the underlying LVLM model can succeed through answer-choice elimination alone.

### B.3. Video-QA Set

As shown in the main paper, PeKit can be extended to video personalization by applying the method to sampled frames. To evaluate this, we used validation video segments (typically under 15 seconds) and curated a VQA dataset with 267 high-quality

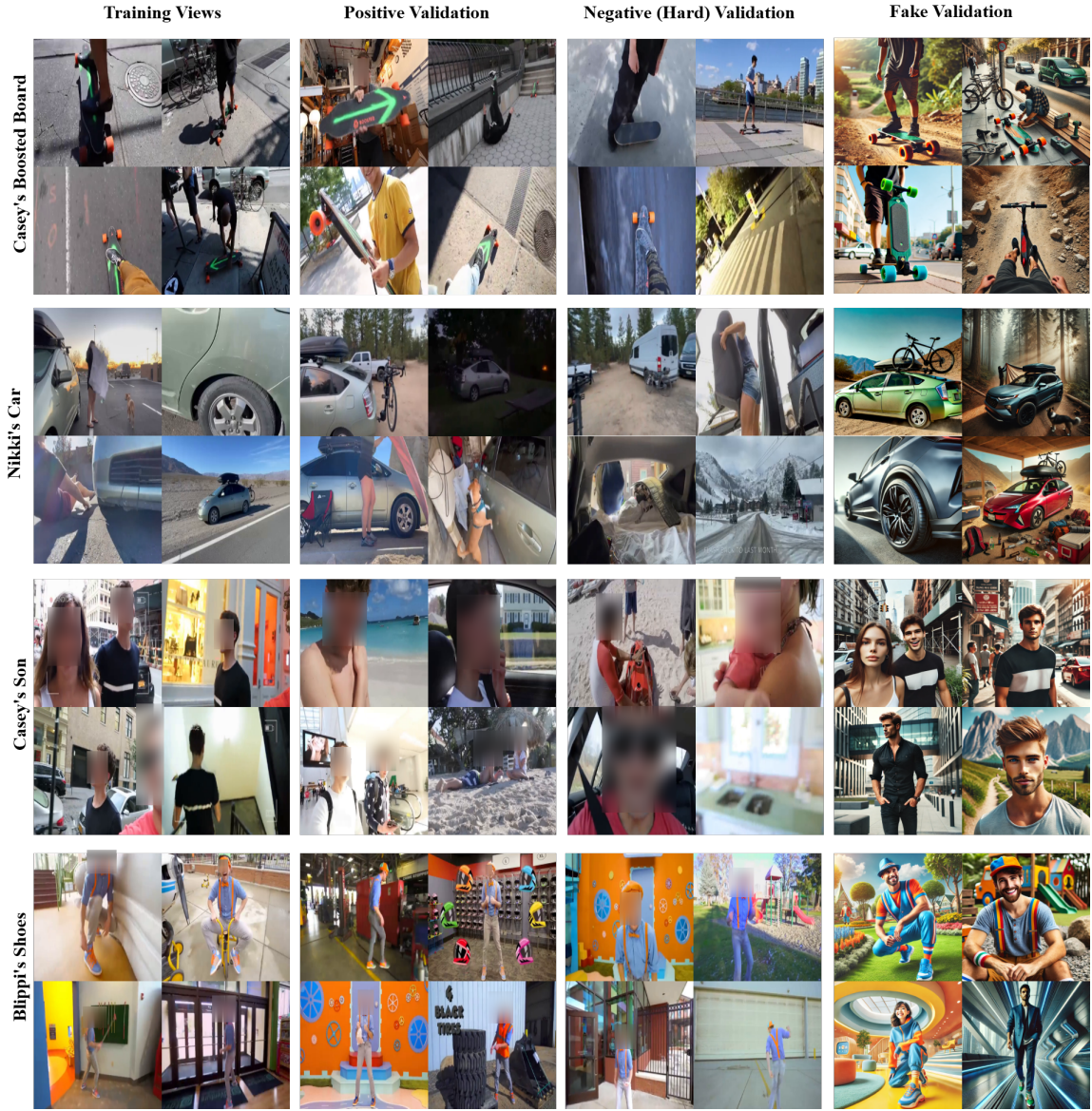


Figure 6. **This-Is-My-Img Single-concept Benchmark.** Our benchmark includes a wide range of concepts presented in realistic indoor and outdoor environments. Reference views can occasionally be sub-optimal, which increases the difficulty of the task. The positive validation set may contain false positives from within the same semantic category, allowing us to assess a model’s robustness to contextual similarities. The negative (hard) and Negative (fake) validation sets are crafted to challenge model resilience by imitating the appearance of personalized objects or their surrounding context. Additionally, the negative (‘other’) set—though not shown in this image—includes images of all other personalized objects for each concept, serving to evaluate the method’s robustness to dataset bias. Faces are blurred to ensure compliance with GDPR.

Category-pair	
Alex - Alex's Bag	Nikki - Nikki's Car
Alex - Alex's Hat	Nikki - Nikki's Camper Bag
Blippi - Blippi's Shoes	Sherry - Sherry's Road Bike
Casey - Casey's Boosted Board	Zak - Zak's Dog Coffee
Casey - Casey's Son	Zak - Zak's Dog Kona
Gab - Gab's Puppy Lili	

Table 10. **Multi-concept Categories on This-Is-My-Img benchmark.** Each category-pair comes with 5 positive frames and 50 negative frames from other category pairs.

question-answer pairs for the single-concept categories in Table 9. For each video segment, we employed the LLaVA-OneVision-Qwen2-7B model with a 1-in-16 frame sampling rate to generate an initial set of 1,380 question-answer candidates. These were then filtered for duplicates using GPT-3.5 Turbo, reducing the set to 618 pairs. Finally, we manually refined the results to produce a curated set of 267 high-quality QA pairs.

## C. Prompt Templates

In this section, we present the specific query format used across different parts of our experiments.

### C.1. Visual prompting

As mentioned in the main paper (Sec 3.4), we employ visual prompting to indicate the personalized object's location in the image. Next we query our LVLM to personalize its answer given the instance's name and context. Our prompt to the LVLM for various tasks follows this general structure:

In this image (video), the entity enclosed in a '**COLOR**' box is called '**NAME**'.

Without mentioning the bounding box and its color, '**TASK**'.

[Optional] Give more details using the information from '**CONTEXT**'.

The **COLOR** placeholder indicates the color of the bounding box overlaid on the image, the **NAME** placeholder specifies the instance name, and the **TASK** placeholder contains the task-specific query. Optionally, the **CONTEXT** place-

holder can contain the prior knowledge about the personalized object retrieved from the memory module.

Note that when multiple objects are detected in one image, the query's grammatical structure changes to a plural format, and the **COLOR** and **NAME** placeholders will contain multiple values separated by commas. The **CONTEXT** placeholder for each object is included in angle brackets (<>) and contains the **NAME** for the corresponding instance.

For the experiments in the paper the **TASK** placeholder can be any of the following prompts:

**Personalized Captioning:** Describe what is '**NAME**' doing. Describe the image too.

**VQA:** Answer the following question about '**NAME**': '**QUESTION**'.

Figure 7 illustrates an example of our full prompt for each one of the tasks.

### C.2. Open-ended VQA Validation

To evaluate the accuracy of model predictions in an open-ended VQA task, we adopt the evaluation pipeline proposed by [19]. In particular, we utilize the following prompt template to query a GPT-3.5-Turbo model for assessing the semantic alignment between predicted answers and ground truth responses for each question in the VQA dataset.

'You are an intelligent chatbot designed for evaluating the correctness of generative outputs for question-answer pairs. Your task is to compare the predicted answer with the correct answer and determine if they match meaningfully.

Here's how you can accomplish the task:

INSTRUCTIONS:

- Focus on the meaningful match between the predicted answer and the correct answer.
- Consider synonyms or paraphrases as valid matches.
- Evaluate the correctness of the prediction compared to the answer.

Please evaluate the following video-based question-answer pair:

Question: **QUESTION**



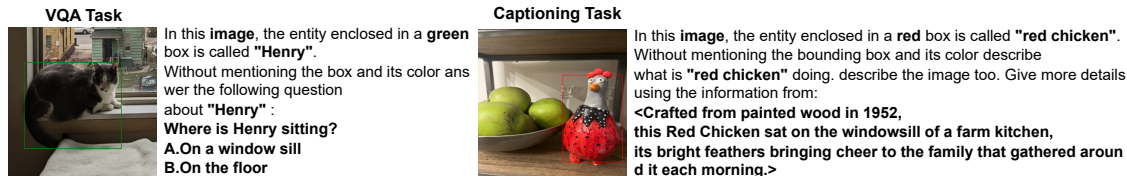


Figure 7. **Prompt Format.** Personalized VQA and captioning on Yo’LLaVA (Left) and MyVLM (Right) datasets. The context used for the ‘red chicken’ is imaginary and generated by ChatGPT.

Correct Answer: **ANSWER**

Predicted Answer: **PREDICTION**

Provide your evaluation only as a yes/no answer.

Please generate the response in the form of a Python dictionary string with key ‘pred’, where value of ‘pred’ is a string of ‘yes’ or ‘no’.

DO NOT PROVIDE ANY OTHER OUTPUT TEXT OR EXPLANATION. Only provide the Python dictionary string. For example, your response should look like this: ‘pred’: ‘yes’.

We calculate the VQA accuracy by dividing the number of times the GPT model, using the specified prompt template, responds with ‘yes’ by the total number of question-answer pairs in the set.

## D. Limitations

In this section we discuss limitations of our method and the room for future research.

### D.1. Wrong Reference Views.

Our approach depends on extracting instance masks through a segmentation network. Noisy or incorrect masks can increase the likelihood of false positives during inference. As shown in Figure 8, noisy masks, overlaid with red on the personalized object, can lead to incorrect matching during inference, depicted with red bounding boxes. Incorporating a clustering method on the extracted reference features to remove the wrong views might enhance the performance of our method by mitigating this issue.

### D.2. Small Objects.

Our method performs feature matching at a resolution lower than the original image due to the

stride factor (=14) in the DINOv2 encoder. This may lead to suboptimal performance for personalized objects that appear small in the reference images. As shown in Figure 9, with a limited number of patches for the personalized object, DinoV2 may not encode enough fine-grained details, capturing only general attributes like the semantic category (e.g., sneakers) or color, which can result in a higher false positive rate. In case the original reference images are available in high resolution, a potential solution is to crop the (small) personalized objects and resize them to DinoV2’s native resolution ( $518 \times 518$ ) before extracting the embeddings.

### D.3. Object Correlations.

Our method, which relies on instance-level detection of personalized objects, could benefit from incorporating contextual information around these objects. This is particularly relevant in scenarios with look-alike objects in contexts that differ from the reference images. For instance, *Alex’s everyday bag* is more likely to appear in an image featuring *Alex* rather than someone else. As a potential future direction, we plan to explore methods for extracting object relationships from reference images and integrating them into our LVLM as prior knowledge.

## E. Qualitative Comparison to LLaVA

Figure 10 presents examples of PeKit model compared to the base LLaVA [17] on VQA and personalized captioning tasks using images from all three benchmarks discussed in the main paper. When LLaVA does not recognize an object from the given name in the query, it makes guesses, leading to hallucinations or incorrect statements. In contrast,

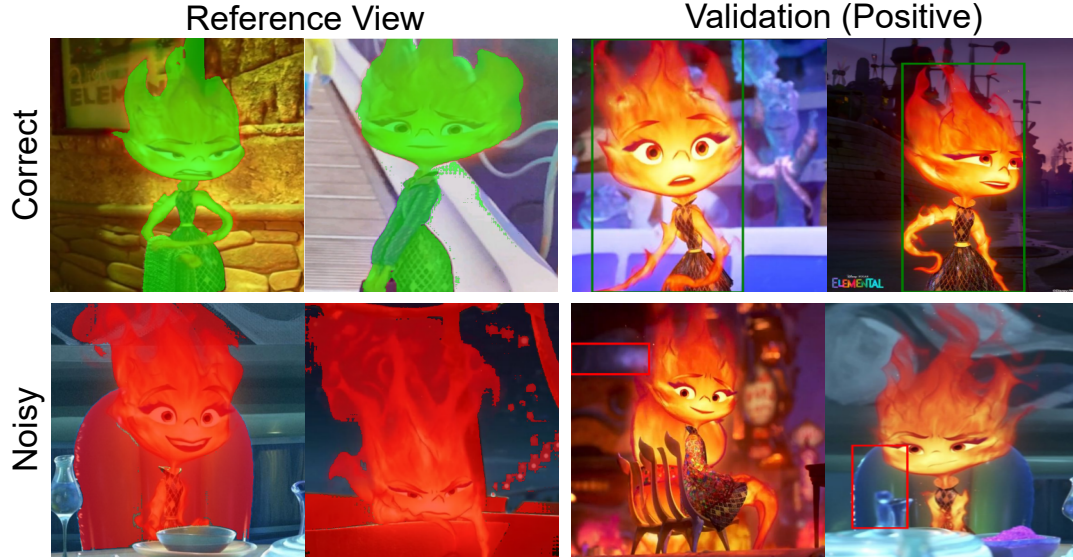


Figure 8. **Noisy Reference Views:** Poor segmentation masks may affect the visual prompting stage and degrade PeKit’s performance.



Figure 9. **Small Reference Objects:** The native image resolution ( $518 \times 518$ ) and stride factor (14) of DinoV2 might result in embeddings of small personalized objects, such as Blippi’s shoes, capturing only general attributes, which can increase the likelihood of false positive detections. The incorrect detections are depicted on our proposed Fake validation set. Faces are blurred to ensure compliance with GDPR.

PeKit accurately identifies objects and uses in-context information to guide LLaVA in answering questions or providing details about the image, effectively incorporating in-context information and object appearance. While more advanced prompting or personalized response examples could en-

hance PeKit, we opted for simplicity and standard design, leaving such improvements for future work.



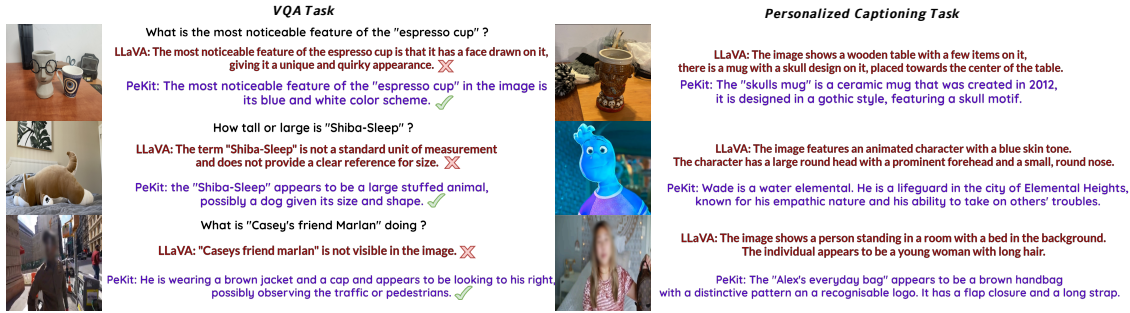


Figure 10. **Comparison to LLaVA**: Right: Our method detects personalized objects and integrates provided context (for qualitative comparison) in caption generation. Left: While the original model struggles with specific questions about named objects, our method easily identifies the referred object. Faces are blurred to ensure compliance with GDPR.

## F. Qualitative Comparison to MyVLM [2]

Figure 11 compares PeKit with MyVLM on images from the MyVLM dataset. We used the original checkpoints and code provided by the authors of MyVLM to generate the results. Checkpoints for the VQA task were not provided.

MyVLM shares the same limitation as Yo’LLaVA, functioning exclusively when the concept identifier is included in the query. Additionally, MyVLM exhibits low precision in detecting personalized objects, as shown in the main paper for the This-Is-My-Img benchmark. This can lead to misidentifying objects as personalized ones. The leftmost image in Figure 11 demonstrates this limitation. MyVLM is asked to provide a caption for the target concept ‘Cat Statue’ while the provided image includes another personalized object, ‘Asian Doll.’ As shown, MyVLM incorrectly identifies the ‘Asian Doll’ as the ‘Cat Statue’ and generates an incorrect personalized caption. Our method addresses this issue by first detecting the correct personalized object(s) and then generating a caption based on the prompt template provided in Appendix C.1.

Furthermore, MyVLM’s training appears to degrade the original LVLM’s captioning capabilities, leading to short captions with hallucinations and sometimes incomprehensible text, leading to a low CLIPScore as demonstrated in the main paper.

## G. Qualitative Comparison to Yo’LLaVA [20]

Figure 12 compares PeKit to Yo’LLaVA for VQA and personalized captioning tasks on This-Is-My-Img benchmark. As seen on the first row, Yo’LLaVA’s prompt template requires the query to include the target object’s concept identifier, making it unsuitable for general captioning tasks and tailored for Visual Question Answering. Besides, since Yo’LLaVA operates on image-level embeddings of reference views, it needs clutter-free object-centered reference views of the personalized objects. As seen on the second row, performance can decline if the personalized object is not in the foreground or if there are other objects/people interacting with the personalized object in the reference views. Besides, fine-tuning the last layer of the language model reduces the LVLM’s captioning capabilities for Yo’LLaVA.

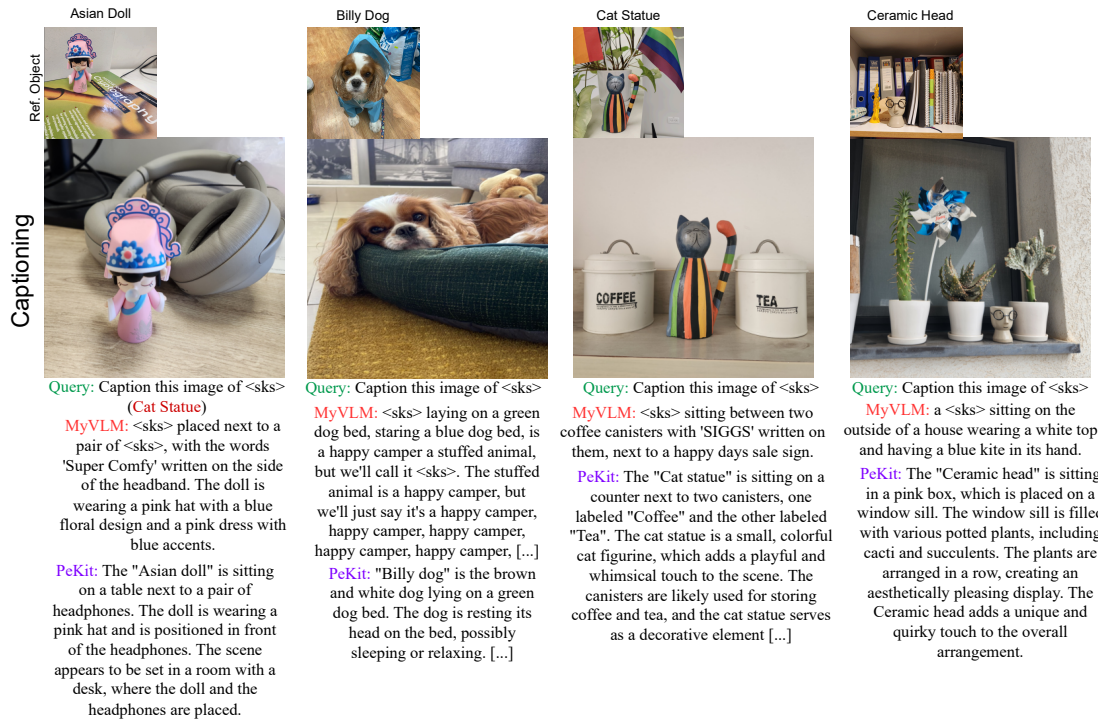


Figure 11. **Comparison to MyVLM:** MyVLM often misidentifies personalized objects because of its low precision. In the leftmost figure, when prompted to caption an image containing a 'Cat Statue'—which is actually absent—MyVLM incorrectly labels the 'Asian doll' and the headset as the 'Cat Statue' instead of rejecting the query. Additionally, MyVLM training interferes with the original captioning capabilities of the LVLM, leading to hallucinations, short captions, and sometimes incomprehensible text. For each image, 'Query' depicts MyVLM's system prompt where the concept identifier <sks> is replaced with the personalized object's name. PeKit employs its own prompt template described in Appendix C.1.

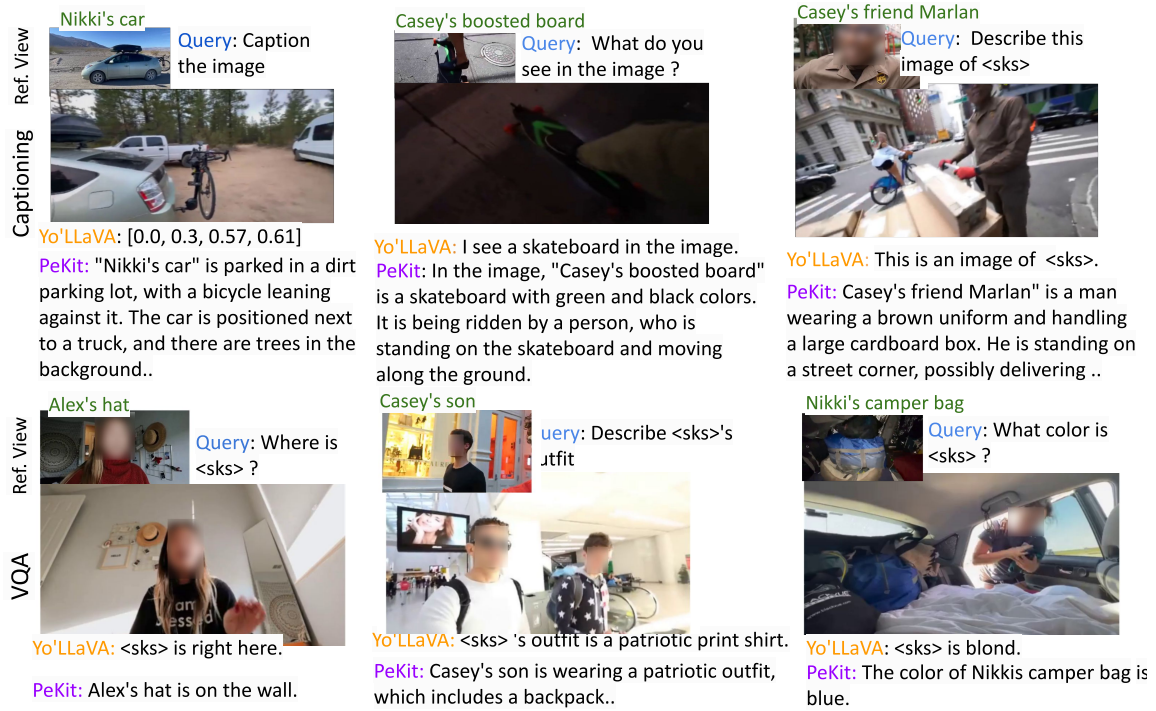


Figure 12. **Qualitative Comparison to Yo'LLaVA:** Yo'LLaVA's prompt template requires specifying the personalized object's identifier in the query (first row), limiting generalization since users must already know which objects are in the image. Using image-level embeddings can also cause confusion between similar objects (e.g., Alex vs. Alex's bag). Adjusting the LLM's head weights further harms captioning quality. PeKit achieves better captioning quality without any training. In each example, the 'Query' shows Yo'LLaVA's prompt with the concept identifier replaced by the object's name and an added system prompt. PeKit uses a different template, detailed in the Appendix C1. Faces are blurred to ensure compliance with GDPR.